Available online at www.sciencedirect.com
SCIENCE DIRECT
Thermochimica Acta 442 (2006) 14–17
thermochimica acta
www.elsevier.com/locate/tca

Simultaneous measurement of specific heat, thermal conductivity, and thermal diffusivity of modified barium titanate ceramics

Kohsuke Morimoto [a,*], Shinya Sawai [a], Kumao Hisano [a], Takashi Yamamoto [b]

[a] *Department of Applied Physics, National Defense Academy, Yokosuka 239-8686, Japan*
[b] *Department of Communications Engineering, National Defense Academy, Yokosuka 239-8686, Japan*

Available online 20 February 2006

Abstract

A radiation calorimeter makes it possible to measure the specific heat, thermal conductivity, and thermal diffusivity of a solid sample simultaneously and independently. Because the three thermal quantities are not independent each other, a self-check of the reliability of the obtained values can also be made from results. Measurements were performed for ferroelectric $BaTiO_3$ ceramics modified with a small amount of Zr, Sn, and Hf in the temperature range of 300–450 K. The modifier content was changed from 2.5 to 12 mol% of Ti ion. Results indicate that the temperature dependence of thermal conductivity changes from crystalline-like to amorphous-like with an increase of content.

Keywords: Barium titanate system; Ceramic; Thermophysical properties; Radiation calorimetry

1. Introduction

Barium titanate is a well-known material because of its ferroelectricity and piezoelectricity. The modification of this material with Zr, Sn, and Hf ions makes the ferroelectric phase transition diffuse. The dielectric properties of $Ba(Ti_{1-x},X_x)O_3$ (X = Zr, Sn, and Hf) associated with ferroelectric phase transition were investigated in detail previously [1–3]. Phase diagrams of these materials were obtained by Matsubara and Yoshimitsu [4]. Recently, the effect of Zr content on the microstructure and dielectric properties was reported for a film [5]. The film of this material has been paid much attention for various applications such as multilayer ceramic capacitors and dynamic random access memories. However, thermo-physical properties of ceramic state of these materials have not yet been investigated as far as present authors are aware. The thermal properties are important from a material design point of view.

Recently, a method based on the thermal radiation calorimetry has been proposed to measure the specific heat, thermal conductivity, and thermal diffusivity of thermal insulating materials simultaneously and independently [6]. In this calorimetry, the temperatures of both surfaces of a disk-shaped sample are measured under quasi-steady-state conditions for heating and cooling modes. The specimen surfaces are blackened to achieve a constant surface emissivity to obtain the radiation power input of the specimen quantitatively. Because the three major thermal properties are not independent each other, a self-check of the reliability of the values obtained from results can be discussed. In this paper, results of measurements on the modified $BaTiO_3$ ceramics are described.

2. Experimental

2.1. Sample preparation

All disk-shaped ceramic samples used in the present experiment were prepared as the following procedure: samples were weighted according to the chemical formula $Ba(Ti_{1-x},X_x)O_3$ (X = Zr, Sn, and Hf). The raw starting materials were chemically pure $BaCO_3$, TiO_2, ZrO_2, SnO_2, and HfO_2. The mixed powders were calcined in an alumina crucible in air at approximately 1400 K for 2 h, 1000 K for 2 h, and 1580 K for 2 h for Zr, Sn, and Hf, respectively. Then the calcined powders were prepared in cylinders under a uni-axial pressure of 10^8 Pa and sintered at 1500 K for 3 h, after milling in a polyethylene container with zirconia balls for 10 h and drying. The structure of these ceramics were identified by powder X-ray diffraction studies and the temperature dependence of dielectric constant was measured to confirm that the ferroelectric transition becomes diffuse with an increase of content. Grain sizes of the ceramics are distributed between 2 and 3 μm and the porosities are

* Corresponding author.

0040-6031/$ – see front matter © 2005 Elsevier B.V. All rights reserved.
doi:10.1016/j.tca.2005.11.020

Table 1
Thickness (d), weight (w), and density (ρ) of modified $BaTiO_3$ ceramic samples

$Ba(Ti_{1-x},Zr_x)O_3$				$Ba(Ti_{1-x},Sn_x)O_3$				$Ba(Ti_{1-x},Hf_x)$			
x (%)	d (mm)	w (g)	ρ (kg/m^3)	x (%)	d (mm)	w (g)	ρ (kg/m^3)	x (%)	d (mm)	w (g)	ρ (kg/m^3)
4	6.45	12.20	5460	2.5	6.98	14.76	5560	4	6.00	12.10	5820
8	8.60	16.38	5500	5	4.02	8.23	5390	8	5.45	11.06	5860
10	7.35	14.06	5520	10	3.02	6.32	5510	10	7.65	15.64	5900
12	9.45	18.03	5510					12	6.00	12.50	6020

less than 1%. The diameters of the samples modified with Zr, Sn, and Hf are, respectively, 21, 22, and 21 mm. The thickness, weight, and density of the samples are listed for various contents in Table 1.

2.2. Theoretical formulation and experimental set-up for radiation calorimeter

We consider the situation in which a disk-shaped specimen is heat on one face slowly by radiation from a flat heater in a vacuum chamber as shown schematically in Fig. 1. An accurate temperature distribution within the specimen is obtained by solving the diffusion equation with boundary conditions and an appropriate initial condition. A linear temperature distribution is obtained for the steady state of the system. For the quasi-steady-state conditions, however, a small temperature deviation from the steady state is obtained by solving the diffusion equation [11], resulting the distribution is parabolic in the direction of thickness. The following relation is derived in this situation [6,7]. That is

$$\lambda\frac{T_L - T_0}{L} = \varepsilon I_0 + \frac{1}{2}C_p\rho L\frac{dT}{dt}, \tag{1}$$

where C_p, λ, ρ, and L denote specific heat, thermal conductivity, sample density, and sample thickness, respectively. T_0, T_L, and dT/dt denote the temperatures of the back surface facing the chamber wall and the front surface facing the heater, and the temperature ramp rate, respectively. ε is the emissivity of back-surface, εI_0 is the radiation power per unit area emitted from back-surface, which is given by $\varepsilon\sigma(T_0^4 - T_r^4)$, where T_r is room temperature and σ is the Stephen constant. The temperature distribution becomes linear for the steady-state conditions and the following equation is derived. That is

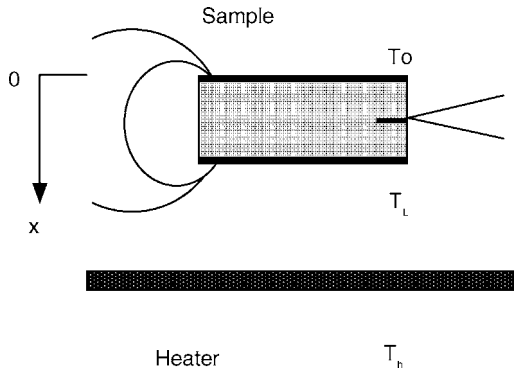

Fig. 1. Schematic set-up of radiation calorimeter. The sample is heat on one face by radiation from a flat heater. The temperature difference between surfaces and the temperature of the centre of side surface are measured using thermocouples.

$$\lambda\left(\frac{T_L - T_0}{L}\right)_{\text{steady}} = \varepsilon I_0. \tag{2}$$

Considering heating and cooling of the system, the thermal diffusivity is given at the same back-surface temperature ($T_0 = T_0'$). That is

$$a = \frac{\lambda}{C_p\rho} = \frac{L^2}{2(T_L - T_L')}\left(\frac{dT}{dt} - \frac{dT'}{dt}\right), \tag{3}$$

where a is the thermal diffusivity. ($'$) means the cooling mode. On the other hand, at the same front surface temperature ($T_L = T_L'$), the specific heat is given by

$$C_p = \frac{E_h(I_h - I_h') - \varepsilon(I_0 - I_0')}{\rho L(dT/dt - dT'/dt)}, \tag{4}$$

where E_h is the effective emissivity depending upon the surface emissivity and the configuration factor between the heater and the sample surface [8]. I_h is the heater emissive power per unit area. Eqs. (1)–(3) imply that the simultaneous measurement of the three thermo-physical properties can be performed by measuring the sample and heater temperatures, the temperature difference between sample surfaces, and the change rate of the sample temperature. Conditions for the quasi-steady state approximation were discussed in detail previously [9]. That is

$$\frac{d(T_L - T_0)}{dt} \ll \frac{12a}{L^2}(T_L - T_0). \tag{5}$$

The plate heater used in the measurements is made with alumina ceramic in which a heater element is suspended. The heater area is 50 mm × 60 mm and the thickness is 1.6 mm. The sample, supported with mullite ceramic tubes (1 mm in diameter), is placed approximately 6 mm above the heater. The sample surfaces were plated with silver metal before blackening. As schematically shown in Fig. 1, a thermocouple set in a hole at the centre of side-surface was used to measure the temperature. Another thermocouples were soldered on both front- and back-surfaces to measure the temperature difference. The heater temperature was measured by use of a thermocouple placed on the centre of the heater. The samples surfaces were blackened with a mixture of powders of Cu_2O, glass, and C, so that the effective emissivity, E_h and the surface emissivity, ε are constant in the present temperature range of 310–450 K. A radiation shield was used to prevent the radiation loss from the sample side surface as much as possible. The entire system was

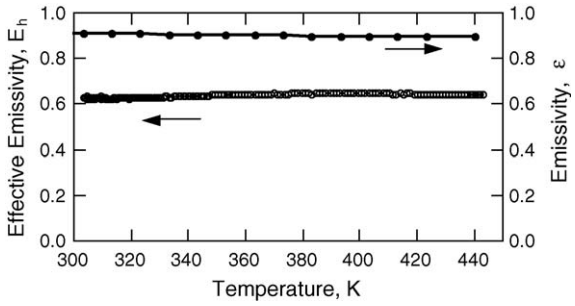

Fig. 2. The effective emissivity, E_h and the surface emissivity, ε. The blackening material is a mixture of powders of Cu_2O, glass, and graphite.

set in a vacuum chamber maintained lower than 10^{-3} Pa. The chamber temperature was kept at 290 K during measurements. Fig. 2 shows the temperature dependencies of the emissivities, E_h and, ε of the blackening material. ε was estimated from the spectral emissivity obtained at 450 K, while E_h was estimated from results using a copper metal sample [1] because its specific heat is well known at various temperatures. As shown in this figure, E_h and ε are constant with a values of 0.62 ± 0.01 and 0.90 ± 0.02, respectively.

3. Results and discussion

Fig. 3 shows the temperature differences between the surfaces of $BaTiO_3$ ceramic for both heating and cooling modes. The ramp rates for both modes are about 2.5 K min^{-1} above 360 K. The hysteresis for both modes reflects the thermal diffusivity as indicated in Eq. (3), while the temperature difference reflects the thermal conductivity as indicated in Eq. (2). The obtained thermal conductivity, λ and thermal diffusivity, a are shown in Fig. 4. The specific heat, C_p is plotted at various temperatures in Fig. 5. The solid lines in Figs. 4 and 5 show the results calculated from other two properties to discuss a self-check of the reliability of the obtained data. Anomalies around 400 K is caused by the ferroelectric phase transition.

As typical examples for modified ceramics, Figs. 6 and 7 plot λ and a of $Ba(Ti_{0.96},Hf_{0.04})O_3$ and $Ba(Ti_{0.88},Hf_{0.12})O_3$ at various temperatures. Similar to Figs. 4 and 5, the solid lines show the results calculated from other two properties. Unlike pure $BaTiO_3$ ceramic, no particular anomalies are found in the temperature dependence even in the vicinity of the transition

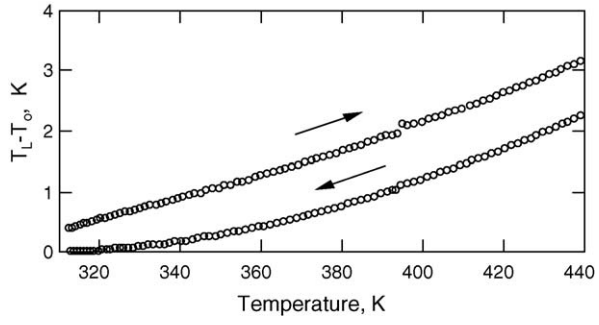

Fig. 3. The temperature difference between the front- and back-surfaces for the heating and cooling modes for $BaTiO_3$ ceramic.

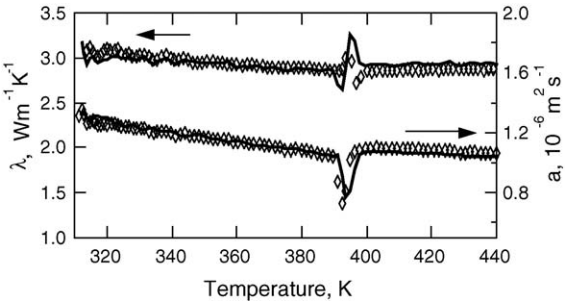

Fig. 4. The thermal conductivity and thermal diffusivity of $BaTiO_3$ ceramic at various temperatures. Open data points are the results obtained experimentally. The solid line in the conductivity shows the results calculated from the diffusivity and specific heat obtained experimentally, while the solid line in the diffusivity shows the results calculated from the conductivity and specific heat obtained experimentally. The conductivity decreases slightly with increasing temperature.

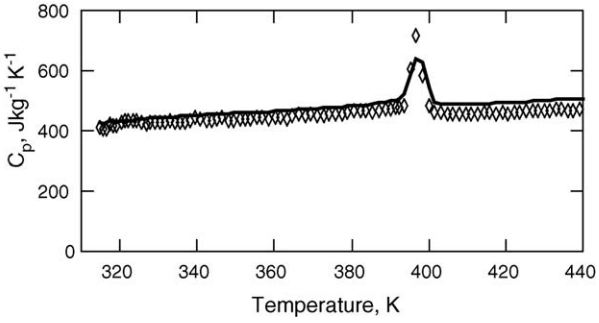

Fig. 5. The specific heat of $BaTiO_3$ ceramic at various temperatures. Open data points are the results obtained experimentally. The solid line is the results calculated from the measured thermal conductivity and diffusivity shown in Fig. 4.

temperature and also λ increases with an increase of temperature for $Ba(Ti_{0.88},Hf_{0.12})O_3$ ceramic. The largest deviations of the calculated values from the experimental values for $BaTiO_3$, $Ba(Ti_{0.96},Hf_{0.04})O_3$, and $Ba(Ti_{0.88},Hf_{0.12})O_3$ are, respectively, 8% in the conductivity and 3% in the specific heat, 4% in the conductivity and 4% in the specific heat, and 9% in the conductivity and 9% in the specific heat. Similar deviations are found in other samples. Relative errors involved in the simultaneous measurements have been estimated as 5%, 10%, and 10% for the specific heat, thermal conductivity, thermal diffusivity, respectively [11]. The deviations of the calculated values are within

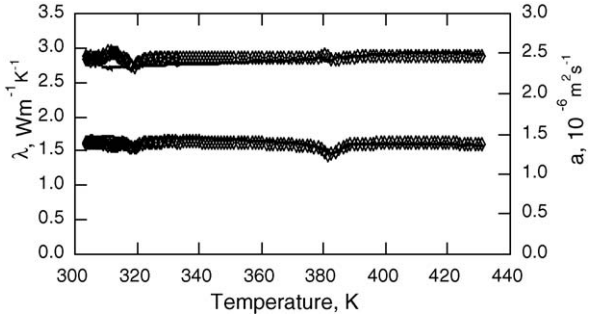

Fig. 6. The thermal conductivity and thermal diffusivity of $Ba(Ti_{0.96},Hf_{0.04})O_3$ ceramic. Open data points are the results obtained experimentally. The solid line is the results calculated from other two properties obtained experimentally. The conductivity is almost independent of temperature.

Table 2
Specific heat, C_p ($J\,kg^{-1}\,K^{-1}$), thermal conductivity, λ ($W\,m^{-1}\,K^{-1}$), and thermal diffusivity, a ($10^{-6}\,W\,m^{-2}\,s^{-1}$) of modified $BaTiO_3$ ceramics. Relative errors involved in the data are 5%, 10%, and 10% for C_p, λ, and a, respectively

$Ba(Ti_{1-x},Zr_x)O_3$				$Ba(Ti_{1-x},Sn_x)O_3$				$Ba(Ti_{1-x},Hf_x)O_3$			
x (%)	C_p	λ	a	x (%)	C_p	λ	a	x (%)	C_p	λ	a
4	326	1.78	1.00	2.5	367	1.90	0.89	4	360	2.89	1.39
8	294	1.82	1.12	5	467	1.68	0.65	8	338	2.14	1.16
10	318	2.55	1.33	10	434	1.25	0.44	10	319	2.16	1.14
12	342	1.71	0.92					12	325	2..20	1.06

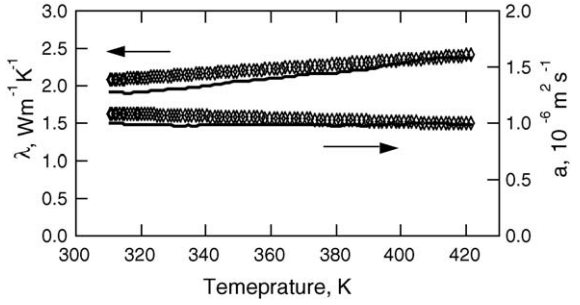

Fig. 7. The thermal conductivity and thermal diffusivity of $Ba(Ti_{0.88},Hf_{0.12})O_3$. Open data points are the results obtained experimentally. The solid lines are the results calculated from other two properties obtained experimentally. The conductivity increases with increasing temperature.

these errors. Fig. 8 shows the thermal conductivity at various modifier contents for the modified samples. Table 2 summarizes values of the three properties obtained at 350 K.

In every present modified system, no particular change in the specific heat was found except the change caused by the ferroelectric phase transition. On the other hand, the temperature dependence of the thermal conductivity changes from crystalline-like to amorphous-like with increasing modifier content except 4% Hf and 10% Zr modified ceramics [10–12]. These materials show almost constant conductivity with temperature. The conductivity of crystalline material generally decreases with increasing temperature, while that of amorphous material increases [13]. Present results seems to be correlated to the fact that the ferroelectric transition becomes diffuse with an increase of modifier content as shown in dielectric constant. In the case of Hf modifier, it is understood that the ceramic becomes amorphous-like above 4% content. However, it is quite hard to explain why the sample modified with 10% zirconium does

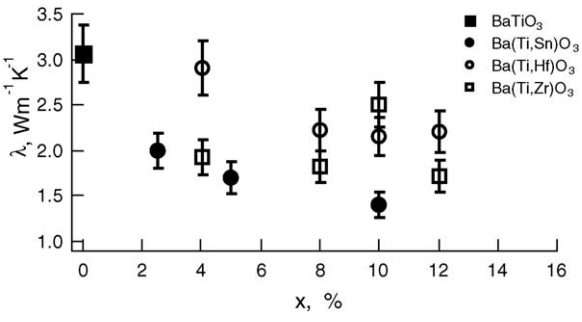

Fig. 8. The thermal conductivities at various modifier contents. Values obtained at 350 K are plotted. Relative errors of 10% are involved in the values.

not show an amorphous-like dependence, although this material shows higher values of conductivity among other samples. No clear explanation for showing an amorphous-like dependence with an increase of content has been performed. More detail investigations on the textile structure of the ceramics such as micro-domains [14], grains, and grain boundaries are particularly required using other experimental techniques to make clear the relation between the diffuse phase transition and the amorphous-like temperature dependence of the thermal conductivity.

4. Conclusion

The specific heat, thermal conductivity, and thermal diffusivity of the Barium titanate system modified with a small amount of Zr, Sn, and Hf were measured simultaneously in the temperature range of 300–450 K by thermal radiation calorimetry. With increasing modifier content, no particular change in the specific heat was found in these materials except the changes caused by the ferroelectric phase transition. On the other hand, the thermal conductivity as well as the thermal diffusivity decreases and its temperature dependence generally becomes amorphous-like. This result seems to be correlated to the diffuse ferroelectric phase transition of the modified system.

References

[1] D. Hennings, A. Schell, J. Am. Ceram. Soc. 65 (1982) 539.
[2] G.A. Smolensky, J. Phys. Soc. Jpn. 28 (Suppl.) (1970) 26.
[3] W.H. Payne, V.J. Tenny, J. Am. Ceram. Soc. 48 (1965) 413.
[4] T. Matsubara, K. Yoshimitsu, Prog. Theor. Phys. 64 (1980) 380.
[5] T. Futakuchi, Y. Nakamura, M. Adachi, Jpn. J. Appl. Phys. 41 (2002) 6948.
[6] K. Hisano, S. Sawai, K. Morimoto, Int. J. Thermophys. 19 (1998) 291.
[7] Japan Patent 2,866,925, Method for Measuring Thermophysical Properties, 2000.
[8] K. Morimoto, S. Sawai, K. Hisano, Int. J. Thermophys. 20 (1999) 709.
[9] S. Sawai, K. Morimoto, K. Hisano, Jpn. J. Appl. Phys. 42 (2003) 6645.
[10] K. Morimoto, A. Uematsu, S. Sawai, K. Hisano, T. Yamamoto, Jpn. J. Appl. Phys. 41 (2002) 6943.
[11] K. Morimoto, Ph.D. Thesis, National Defense Academy, Japan National Institution for Academic Degrees and University Education, 2004.
[12] K. Morimoto, S. Sawai, K. Hisano, T. Yamamoto, Jpn. J. Appl. Phys. 42 (2003) 6196.
[13] S.R. Elliott, Physics of Amorphous Materials, Longman, London and New York, 1984.
[14] L.E. Cross, Ferroelectrics 76 (1987) 241.